Petroleum Science 19 (2022) 1964–1977

Contents lists available at ScienceDirect

Petroleum Science

journal homepage: www.keaipublishing.com/en/journals/petroleum-science

Original paper

Vertical grain-size trend of mouth bar in lacustrine fan delta: Flume experiments

Ke Zhang [a, b], Sheng-He Wu [a, b, *], Jun-Jie Wang [a, b], Yun-Jie Xu [a, b], Zhen-Hua Xu [c], Jia-Jia Zhang [a, b]

[a] State Key Laboratory of Petroleum Resources and Prospecting, China University of Petroleum (Beijing), Beijing, 102249, China
[b] College of Geosciences, China University of Petroleum (Beijing), Beijing, 102249, China
[c] School of Geosciences, Yangtze University, Wuhan, Hubei 430100, China

ARTICLE INFO

Article history:
Received 21 July 2021
Accepted 28 February 2022
Available online 6 April 2022

Edited by Jie Hao

Keywords:
Mouth bar
Vertical grain-size trend
Effluent behavior
Inertia
Bed friction

ABSTRACT

Field observational previously indicated a mouth bar of a fan delta could exhibit a fining- or coarsening-upward trend, which bring a new challenge to the identification of mouth bar in subsurface studies due to the lack of morphological descriptions. Previous studies have indicated that effluent behavior in river-mouth system can affect the vertical grain-size trend of mouth bar, but the drivers and magnitude of this phenomenon are not understood. We conducted flume experiments to investigate the mechanism and controlling factors of vertical grain-size trend of mouth bar. Experiment with a steeper slope of the substrate layer, greater discharge, higher sediment/water ratio, and coarser sediment induced a fining-upward trend of mouth bar, because the effluent was dominated by strong inertia. Mouth bar in the experiment with a gentler slope of the substrate layer, smaller discharge, lower sediment/water ratio, and finer sediment exhibited a coarsening-upward trend dominated by the friction-dominated effluent. The relationship between the vertical grain-size trend of mouth bar and the gradients of foreset bedding in small-scale flume models and the cut-off of 15°–18° are applicable in natural systems. Identifying depositional setting to infer depositional process in river-mouth system and analyzing the plane geometry of sandbodies are two steps in the interpretation of ancient fan deltaic rock record.

1. Introduction

Mouth bar, as an important element of delta systems, deposits at the channel mouth because of the decrease in jet momentum during the transition from channelized flow to unconfined flow (Wright, 1977; Edmonds and Slingerland, 2007, 2010; Hoyal and Sheets, 2009; Paola et al., 2011; Fagherazzi et al., 2015). The description of morphology, facies associations, and vertical grain-size trends laid the foundation for the distinction of mouth bars from other deposits in field observational studies (Heerden and Roberts, 1988; Ilgar and Nemec, 2005; Fielding et al., 2005; Bressan et al., 2013; Fabbricatore et al., 2014; Carvalho and Vesely, 2017). However, the morphological characteristics of mouth bar were not analyzed in subsurface studies without seismic data. The facies associations and related vertical grain-size trend, which were descriptive based on core analysis and logging data only, are significant for identification of mouth bar (Xu et al., 2015; Ambrosetti et al., 2017; Lai et al., 2017; Nian et al., 2018; Leila and Moscariello, 2019; Wu et al., 2020).

The river-mouth environment causes the formation of diamond-shaped mouth bars in fluvial deltas, flanked by bifurcating distributary channels. There is a general consensus that mouth bar of fluvial delta shows an overall coarsening-upward trend (Van Herdeen and Robert, 1988; Tye and Coleman, 1989; Bhattacharya and Willis, 2001; Schomacker et al., 2010). However, the vertical grain-size trend of mouth bar in fan delta is still a debatable topic. Works based on outcrop or subsurface data have recognized the mouth bar of fan delta with coarsening-up successions (Billi et al., 1991; García-García et al., 2006; Jia et al., 2018). This is the same as grain-size trend of mouth bar in fluvial delta. Conversely, a few other works utilized outcrop studies and reported the fining-upward mouth bars in fan deltaic successions.

* Corresponding author. State Key Laboratory of Petroleum Resources and Prospecting, China University of Petroleum (Beijing), Beijing, 102249, China.
E-mail address: reser@cup.edu.cn (S.-H. Wu).

https://doi.org/10.1016/j.petsci.2022.03.024

Specifically, Benvenuti (2003) focused on facies analysis and depositional architecture of fan delta located at the Pliocene-Pleistocene Mugello Basin and argued that mouth bar showed an overall fining-upward trend. The mouth bar of fan delta consists of massive, weakly normally graded, cobble-bearing pebble gravel overlain by low-angle, cross-stratified, medium- or fine/medium-grained sand and commonly capped with a planar parallel-stratified, fine/medium-grained sand. In addition, Fabbricatore et al. (2014) presented that proximal mouth bar conglomerates of fan delta in Pleistocene Crati Basin are characterized by repeated fining-upward packages, and distal mouth bar conglomerates and sandstones are normally graded, rarely showing inverse grading. Distinguishing the mouth bar deposits of fan delta from distributary channels in rock record may not be as straightforward as often portrayed, because the vertical grain-size trend of mouth bar can be more variable than usually presumed.

Apart from describing the vertical grain-size trend of mouth bar in fan delta, the mechanism and controlling factors of the vertical grain-size trend have attracted the attention of geologists. The inverse grading of deposits with sharp, non-erosive bed contacts, reflecting the presence of intergranular dispersive pressure, are likely related to noncohesive debris flows (Shultz, 1984; Rasussen, 2000; Rohais et al., 2008). A normal gradient of lobes in fan delta system is controlled by a coarse-grained granular flow, driven by inertial forces under conditions of excess pore pressure (Mutti et al., 2000). The fining-upward trend of mouth bar in Mugello Basin is thought to be the subaqueous product of unconfined flash floods in channel-mouth conditions, where inertial expansion of the flood flow occurred in the lake water (Benvenuti, 2003). Based on the results of flume experiments, Wang et al. (2015) explained that coarser sands were deposited at proximal parts of the mouth bar due to friction-dominated effluent diffusion model presented by Wright (1977). The mouth bar developed retrogradely, causing the finning-upward sequence of mouth bar. All these studies suggest that the deposition process and flow dynamics can potentially affect the vertical grain-size trend of mouth bar, but the magnitude and drivers of this influence are not understood. This gap hampers the identification of mouth bars in subsurface reservoir studies.

The mouth bar was developed due to fan delta progradation (Van Dijk et al., 2009; Zhang et al., 2016; Miller et al., 2019), in a manner similar to the development of mouth bar in fluvial delta environment, bar in braided river and other deposits with cross-stratification (Edmonds and Slingerland, 2010; Schuurman et al., 2013; Caldwell and Edmonds, 2014; Weckwerth, 2018; Zhang et al., 2020). Neglecting the influence of tidal range and incident wave power, effluent behavior and consequent depositional patterns depend on the relative dominance of inertia, bed friction and buoyancy in river-mouth system where the mouth bar deposited (Wright, 1977). Inertia or bed friction is dominant in lacustrine basin, rather than buoyancy, as buoyancy-dominated depositional pattern commonly occurs when the fresh water spreads as a buoyant plume above the underlying salt water (Wright and Coleman, 1974). Coarser sands with greater inertia are deposited at distal parts of foreset bedding, and conversely finer sands deposited at proximal parts in inertia-dominated depositional pattern, resulting in the fining-upward trend of mouth bar. Whereas coarser sands with greater friction due to greater weight are deposited upstream, while finer sands are deposited at distal parts of foreset bedding in bed friction-dominated depositional pattern (Coleman et al., 1964; Arndorfer, 1973; Wright, 1977; Postma, 1990), resulting in the inverse grain-size trend (Zavala and Pan, 2018).

The effluent behavior in river-mouth system is associated with the grain size distribution along the foreset bedding, which is strongly associated with the vertical grain-size trend of the mouth bar. However, the controlling factors of effluent behavior are not yet understood. This study conducted flume experiments to elucidate the mechanism and controlling factors of the vertical grain-size trend of a mouth bar of a fan delta. The controlled experiment was conducted for different slopes of substrate layer and different feeder systems, such as discharge, sediment/water ratio and median grain size of sediments. The objectives of the study are to (1) determine the trends of the mouth bars of the fan delta, (2) elucidate what affected the behavior of the river-mouth system, and (3) validate small-scale flume tank models by observational data. The misinterpretation of fining-upward mouth bar as distributary channel in rock record could be avoided by understanding the formation mechanism of fining-upward mouth bar.

2. Experimental design

2.1. Flume set-up and materials

The experiments of this study were first reported by Zhang et al. (2021). Specifically, the ten fan delta experiments (R1–R10) were conducted at the Flume Facility at Yangtze University, Wuhan, China. The experimental arrangement consisted of a 5cm-wide, 0.8 m-long alluvial river, which drained into a horizontal basin (2.16 m × 2.25 m). Above the flat basement floor of the basin, we laid down an initial substrate layer of coarse sand for the fan delta to build out onto. Sediment was delivered at a constant rate from a hopper with a rotating helix and was mixed with the water supply before entering the alluvial river. The alluvial river dimensions ensured that the flow entered the basin as a steady and centered jet (Van Dijk et al., 2009; Zhang et al., 2016). The base level, controlled by a pump that drained water into the drainage pond, was held constant throughout the experiment above the substrate layer (Fig. 1). Sediments were obtained from a natural river, while the grain-size range of sediment is between 0.072 and 3000 μm. The grain-size distribution of sediments in the experiments is shown in Fig. 2. Input conditions and other variables are listed in Table 1. R1–R3 experiments were performed for different substrate layer slopes and water depths. The water depth difference stemmed from the substrate layer slope difference. R4–R6 experiments were carried out with different discharges, whereas the R5, R7, and R8 experiments were carried out with different sediment/water ratios (Q_s/Q_w). Lastly, the R4, R9, and R10 experiments were carried out with different median grain sizes of sediment.

2.2. Experimental data collection

In this study, we recorded the grain size distribution of the fan delta and prograded slopes of mouth bar to examine the vertical grain-size trend of mouth bar, which is related to its deposition process. According to the flume experiments of fan delta process by Van Dijk et al. (2009), the channelization of the flow was accompanied by transient mouth bar deposition at the tips of the channel. In particular, the confined channel flow with enhanced transport capacity deposited the sediment in a rapidly prograding fan delta lobe, followed by the development of a distinct mouth bar along the centerline (Fig. 3). On this basis, we selected the fan delta profile along centerline to measure the slopes of foreset bedding as mouth bars deposited along the centerline were large-scale ones (Fig. 4d). The samples for grain size analysis are selected from the proximal, middle and distal parts of fan delta and from the profile of fan delta along the centerline (Fig. 4a–c). The samples from the proximal, middle and distal parts of fan delta were evenly distributed in both vertical and horizontal directions. Besides, the samples from fan delta profile along the centerline were evenly distributed along foreset bedding of mouth bars (Fig. 4d). Note that the median grain

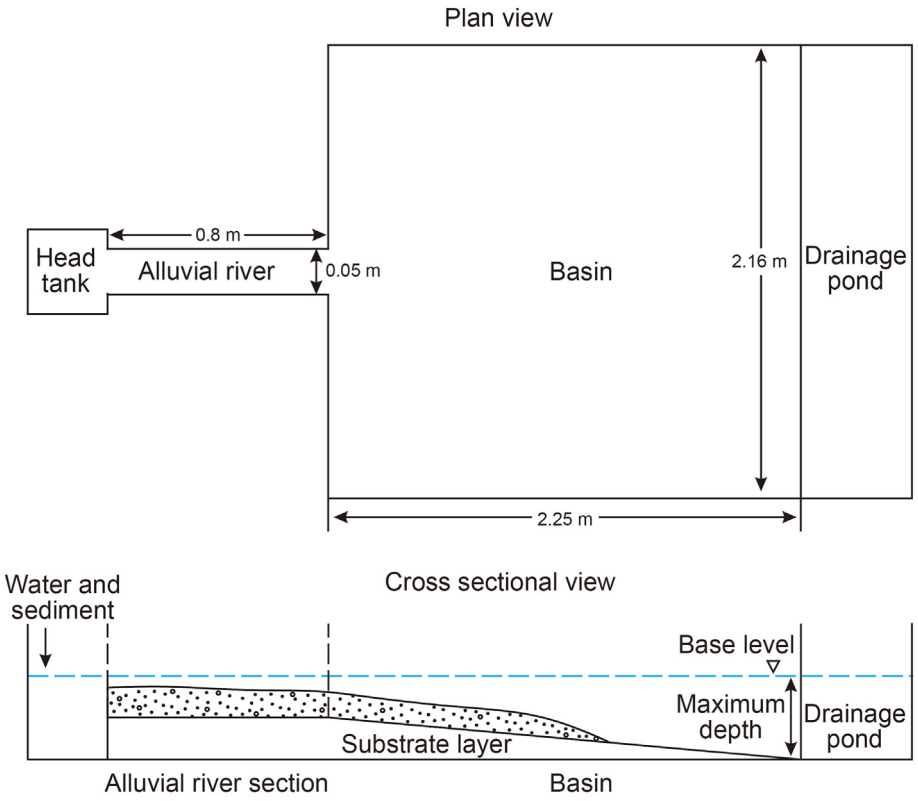

Fig. 1. Schematic view of the experimental set-up.

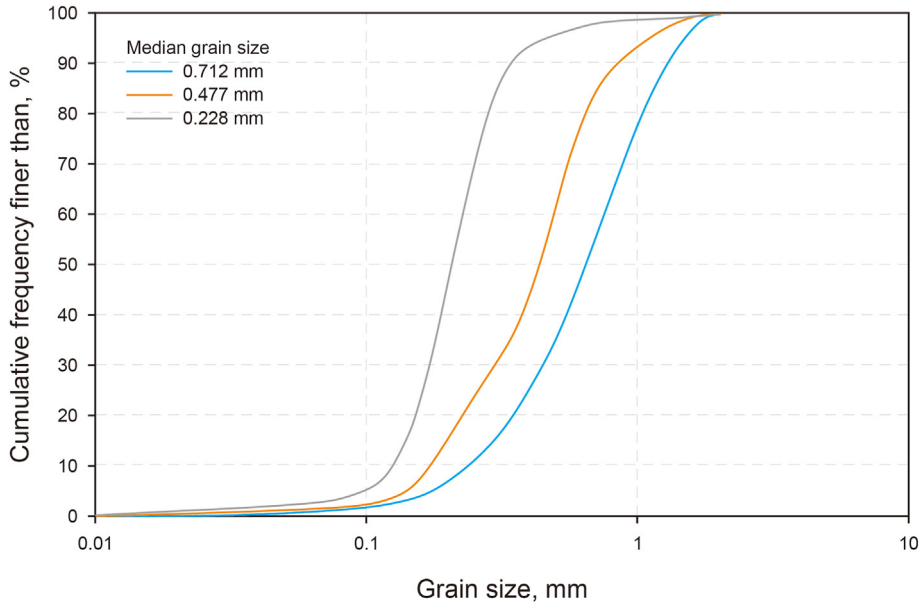

Fig. 2. Grain size distribution of sediment used in the experiments (according to Zhang et al., 2021).

size of sample from the top and bottom of mouth bar is hereafter referred to as G_t and G_b, respectively. All the grain size analyses were conducted using an electric vibrating sieving machine and LS I3 320 Laser diffraction particle size analyzer at the Experimental Research Center of School of Geosciences, Yangtze University. Additionally, we recorded the crucial parameters for quantitative analysis of vertical grain-size trend of mouth bar. Specifically, the D_f is defined as the horizontal distance between alluvial river outlet and the end of foreset bedding, and L is defined as the length of foreset bedding (Fig. 4d). The rate of grain size change along the foreset bedding is defined as the grain size difference per foreset bedding length $((G_b-G_t)/L)$.

Table 1
Input conditions of experiments. The blue areas (from R1–R3 experiments) represent experiments carried out with different substrate layer slopes and water depths. The water depth difference resulted from the substrate layer slope difference. The red areas (from R4–R6 experiments) represent experiments carried out with different discharges. The yellow areas (R5, R7, and R8 experiments) represent experiments carried out with different sediment/water ratios (Q_s/Q_w). The green areas (R4, R9, and R10 experiments) represent experiments carried out with different median grain sizes of sediment (according to Zhang et al., 2021).

Experiment	Slope of substrate layer	Maximum water depth, cm	Sediment supply, Q_s, $m^3 h^{-1}$	Discharge, Q_w, $m^3 h^{-1}$	Q_s/Q_w ratio	Median grain size of sediments, μm
R1	0.005	6	0.01125	0.360	0.03125	712
R2	0.025	10	0.01125	0.360	0.03125	712
R3	0.050	15	0.01125	0.360	0.03125	712
R4	0.025	5	0.01125	0.360	0.03125	477
R5	0.025	5	0.00788	0.252	0.03125	477
R6	0.025	5	0.00338	0.108	0.03125	477
R7	0.025	5	0.0045	0.252	0.0179	477
R8	0.025	5	0.00225	0.252	0.0089	477
R9	0.025	5	0.01125	0.360	0.03125	228
R10	0.025	5	0.01125	0.360	0.03125	712

The entire fan delta processes are recorded using a digital camera and a 3D laser scanner. The digital camera is set above the tank and images are taken at 1-min intervals. The 3D laser scanner is mainly composed of laser emitter, receiver, time counter and rotatable filter controlled by motor. 3D laser scanning technology can provide 3D point cloud data of scanned object surface, so it can be used to obtain high-resolution digital terrain model. The surface topography is measured using the faro focus s70 3D laser scanner in our tank experiments, and both vertical and horizontal resolutions were 0.01 mm. The flow velocity estimates are based on instantaneous flow depth measurements, using digital elevation data for bed elevation in channel cross-sections and photographs for determining the wetted width.

3. Results

3.1. Vertical grain-size trend of mouth bar

The mouth bars of fan delta mostly show the fining-upward trend in experiments, only a few columns in R6-R9 shows the coarsening-upward trend (Fig. 5, Table 2). According to the grain size distribution along foreset bedding and vertical grain size distribution, the grain size gradually increases along forest bedding within the fining-upward foresets, whereas the grain size gradually decreases along forest bedding within the coarsening-upward foresets. Furthermore, the prominent vertical grain size distribution is associated with apparent differences in grain size distribution along foreset bedding (Fig. 5a). Thus, the vertical grain-size trend of the mouth bar is strongly connected to grain size variation along foreset bedding.

The fan delta process consists of period of original jet flow, sheet flow, and cyclical alternations of several small secondary channelized flows and fully confined channelized flow (Zhang et al., 2021). During the period of several small secondary channelized flows, sediment was transported by small radial secondary channels and deposited at the shoreline. Mouth bars related to several small secondary channels show the different ranges of grain size distribution because of different transportation ability of several small secondary channels and different distances travelled. It is challenging to quantify the vertical grain-size distribution of the mouth bar associated with the small secondary channels, observed from Columns, regardless whether a single experiment or all the experiments are considered. However, the fluid converged from steeper flanks to the centerline during the period of the fully confined channelized flow. The mouth bar, which is related to the confined flow, formed only along the centerline. Thus, the mouth bar developed along the centerline is preferred for vertical grain-size distribution studies. As the vertical grain-size trend of the mouth bar is consistent with the grain-size variation along the foreset bedding and the presence of more samples along the foreset bedding, we quantified the vertical grain-size distribution of mouth bar along the centerline. To this end, we compared the grain-size distribution along the foreset bedding.

The grain size distribution along the foreset bedding for the experiments are shown in Fig. 6. Yellow circles and orange circles represent the median grain size of samples of the top and bottom of mouth bar, respectively. The length of lines (blue, green and gray) between circles represent the range of median grain size change along the foreset beddings. As D_f gradually increases, both the median grain size of samples and its range show a decreasing trend within the fining-upward foresets, whereas the range of median grain size increases slightly within the coarsening-upward foresets. Moreover, the grain-size range of mouth bar increases with the increase of slope of substrate layer, discharge, sediment/water ratio and median grain size of sediment supplied.

The definition of the rate of grain size change along the foreset bedding implies that its positive value reflects the increasing trend of grain size along foreset bedding and fining-upward trend of mouth bar. Conversely, a negative value reflects a decreasing trend of grain size along foreset bedding and coarsening-upward trend of mouth bar. As shown in Fig. 7, most values of it are positive. The rate of grain size change along the foreset bedding shows a decreasing trend as the D_f gradually increases. It also decreases with a reduction in the slope of substrate layer, discharge, sediment/water ratio and median grain size of sediment supplied (Fig. 7).

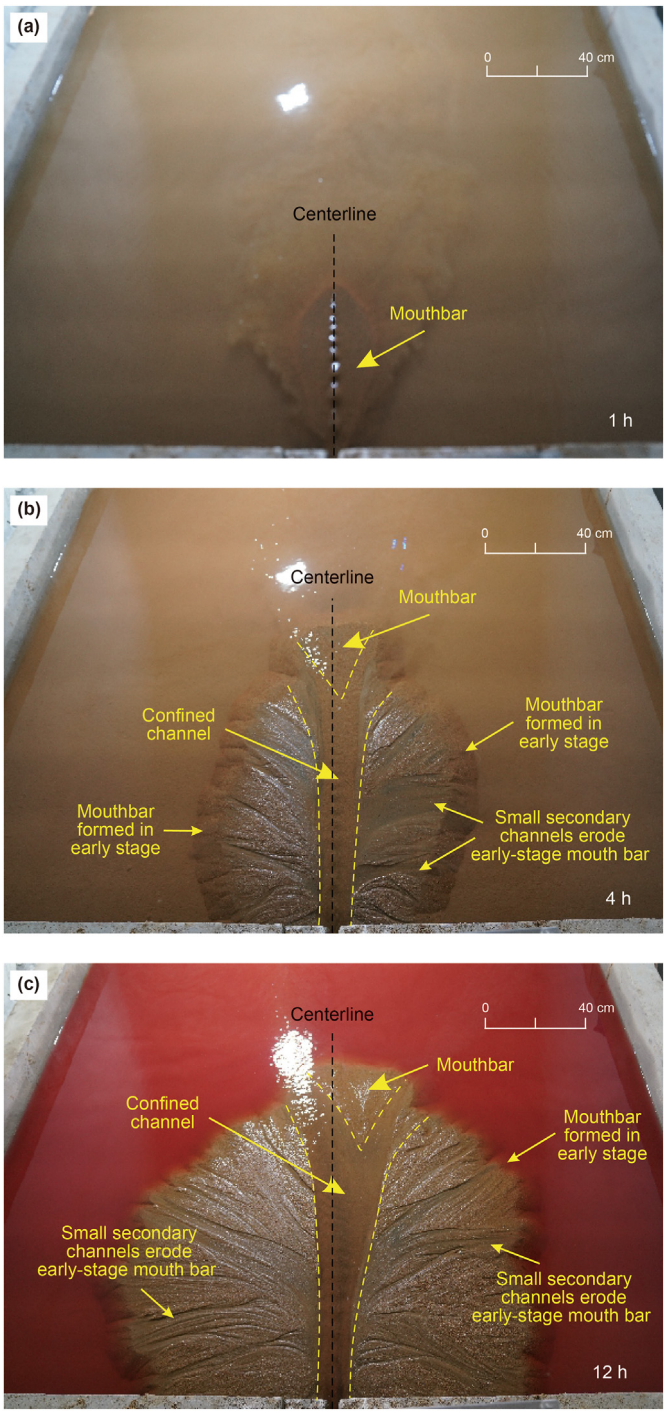

Fig. 3. The confined channel flow with enhanced transport capacity deposited the sediment in a rapidly prograding fan delta lobe, followed by the development of a distinct mouth bar along the centerline. Mouth bars deposited along the centerline during the periods of fully confined channelized flow is much larger than the mouth bars deposited during the periods of several small secondary channelized flows.

3.2. Gradients of foreset bedding

In previous studies of vertical grain size distribution of mouth bar, the angle of clinoform set was referred constantly (Wright, 1977; Postma, 1990; Fielding et al., 2005). The mouth bars with the different vertical grain-size distributions exhibited variable inclined characteristics, but the quantitative relationship between them is unclear. Due to this, we quantified and analyzed the foreset bedding gradients in the experiments. During the evolution of fan delta, the gradients of foreset bedding clearly show a decreasing trend in each experiment, despite the gradient building up slightly sometimes (Figs. 8 and 9). The gradients of foreset bedding from experiment R3 were the steepest, ranging from 25.86° to 32.86° and averaging 29.04°, whereas the gradients from experiment R6 were the gentlest, ranging from 19.93° to 17.43° and averaging 18.805° (Table 3). Besides, we identified the significant differences in gradients of the foreset bedding for the experiments with different slopes of substrate layer and feeder systems. The R1–R3 experiments indicated that the gradients of foreset bedding increased with increasing slope of the substrate layer at the same distance from the alluvial river outlet, although the maximum gradient of foreset bedding measured in experiment R1 was steeper than the gradient for experiment R2 (30.28° and 29.43°, respectively). The average gradients of foreset bedding were 24.56°, 25.84° and 29.04° for experiments R1, R2 and R3, respectively (Fig. 10a). The experiments R4–R6 revealed the following pattern: the gradients of foreset bedding decreased with decreasing discharge at the same distance from alluvial river outlet. In the experiments R4, R5 and R6, the measured gradient of foreset bedding varied from 24.93° to 22.43° (averages 23.73°), 24.03° to 20.43° (averages 22.56°) and 19.93° to 17.43° (averages 18.81°), respectively (Fig. 8b). In spite of the gradients of foreset bedding we measured for experiment R7 was the gentlest among experiments R5, R7 and R8, taking account of the difference of distance between the foreset bedding we measured and alluvial river outlet, gradients of foreset bedding decreased from experiment R5 to R7 and R8 with decreasing sediment/water ratio (Fig. 10c). From experiment R10 to R4 and R9, gradients of foreset bedding decreased with decreasing median grain size at the same distance from alluvial river outlet. The maximum gradients of foreset bedding were 26.43°, 24.93° and 21.43° for experiment R10, R4 and R9, respectively, whereas the average gradients were 23.36°, 23.73° and 19.56°, respectively (Fig. 10d).

4. Discussion

4.1. Controlling factors of the vertical grain-size trend of mouth bar

The cross plot revealed a strong positive relationship between gradient of foreset bedding and the rate of grain size change along foreset bedding, with R^2 value of 0.8477 within the fining-upward foresets and R^2 value of 0.8427 within the coarsening-upward foresets (Fig. 11). The absolute values of rate of grain size change indicate the range of grain size distribution along foreset bedding. Apparent difference in the grain size distribution makes great absolute value. Thus, gentler foreset bedding is associated with wide range of grain size distribution along foreset bedding when the mouth bar shows the coarsening-upward trend, and steeper foreset bedding is connected to the great difference in grain size distribution when the mouth bar shows the fining-upward trend. Moreover, Fig. 11 shows that the foreset bedding gradients are less than 20° within coarsening-upward trend of mouth bar, whereas the gradients are mainly greater than 20° within fining-upward trend of mouth bar, which is similar to the findings of other physical modeling conducted by Muto et al. (2012), Burpee et al. (2015), Wang et al. (2015) and Miller et al. (2019). We counted the gradients of foreset bedding and corresponding vertical grain-size trend of deposits they described in their published papers, and the results indicate that mouth bars with low angle foresets (gentler than 15°) are associated with coarsening-upward profiles, whereas mouth bars with steep foresets (steeper than 18°) are associated with fining-upward successions. Mouth bar showed

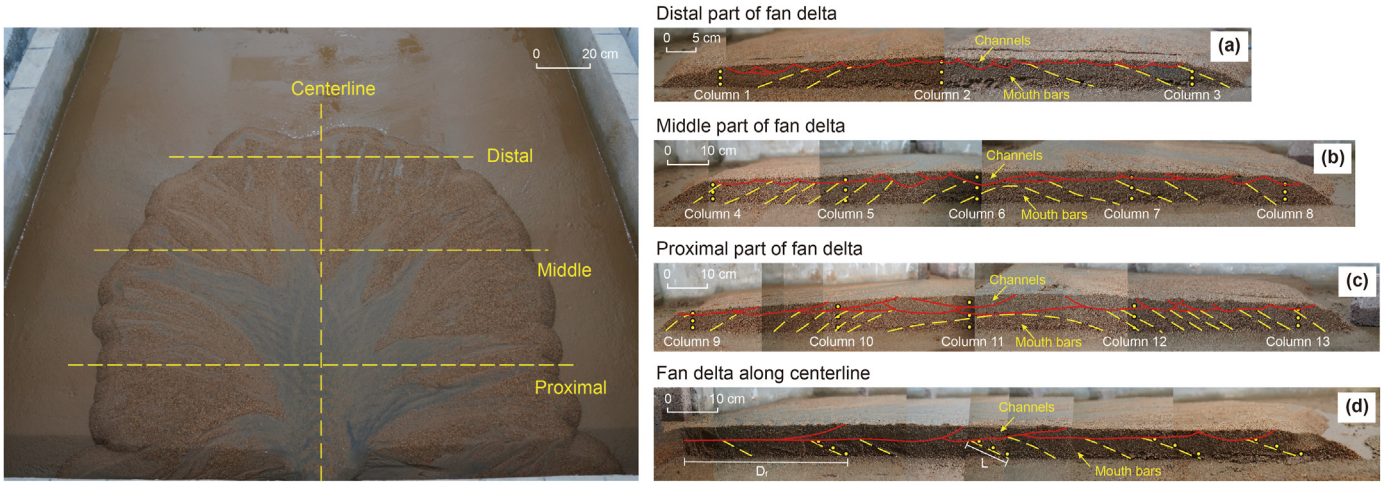

Fig. 4. Samples selected for grain size analysis and definitions of D_f and D_s. The yellow spots represent the locations of sample selection. Red and yellow lines represent the channels and foreset bedding of mouth bar, respectively. The samples from the proximal, middle and distal parts of fan delta were evenly distributed in both vertical and horizontal directions. Besides, the samples from fan delta profile along centerline were evenly distributed along foreset bedding of mouth bars. The D_f is defined as the horizontal distance between alluvial river outlet and the end of foreset bedding, and L is defined as the length of foreset bedding.

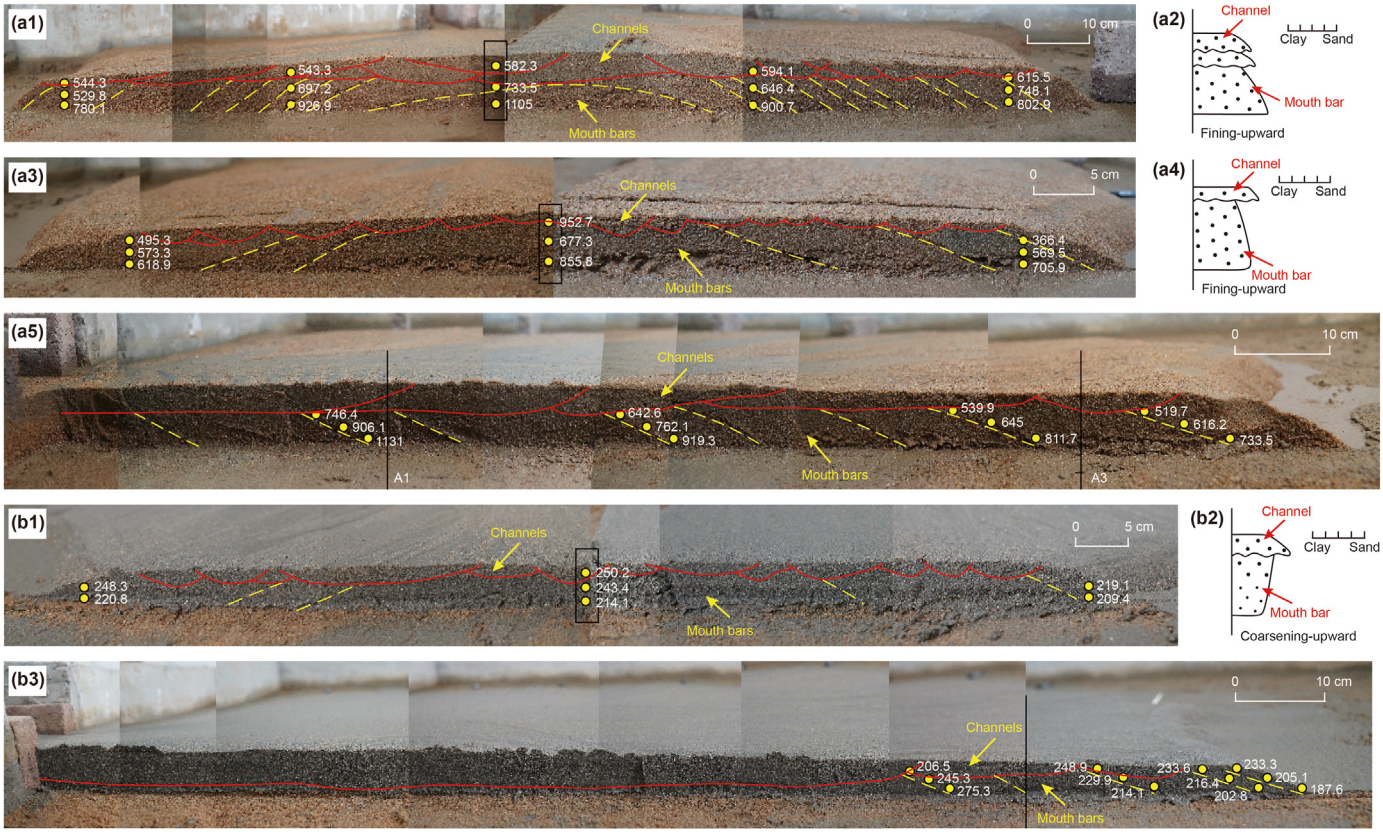

Fig. 5. Vertical grain size of mouth bar. a: Fining-upward trend of mouth bar. The grain size gradually increases along forest bedding within the fining-upward foresets (a1: Proximal part of fan delta of experiment R1. a2: Detailed sedimentological logs of rectangular zone in a1. a3: Distal part of fan delta of experiment R1. a4: Detailed sedimentological logs of rectangular zone in a3. a5: Fan delta profile along centerline of experiment R1. Black line in a5 represents the cross-section locations of a1 and a3). b: Coarsening-upward trend of mouth bar. The grain size gradually decreases along forest bedding within the coarsening-upward foresets (b1: Distal part of fan delta of experiment R9. b2: Detailed sedimentological logs of rectangular zone in b1. b3: Fan delta profile along centerline of experiment R9. Black line in b3 represents the cross-section location of b1). The numbers near the sample represent the median grain size of samples, μm.

Table 2
The vertical grain size trend of mouth bar.

Experiment	Fining-upward trend	Coarsening-upward trend
R1	Column 1–13	/
R2	Column 1–13	/
R3	Column 1–13	/
R4	Column 1–13	/
R5	Column 1–13	/
R6	Column 5–7, Column 9–13	Column 1–4, Column 8
R7	Column 4–13	Column 1–3
R8	Column 5–7, Column 9–13	Column 1–4, Column 8
R9	Column 5–7, Column 10–12	Column 1–4, Column 8–9, Column 13
R10	Column 1–13	/

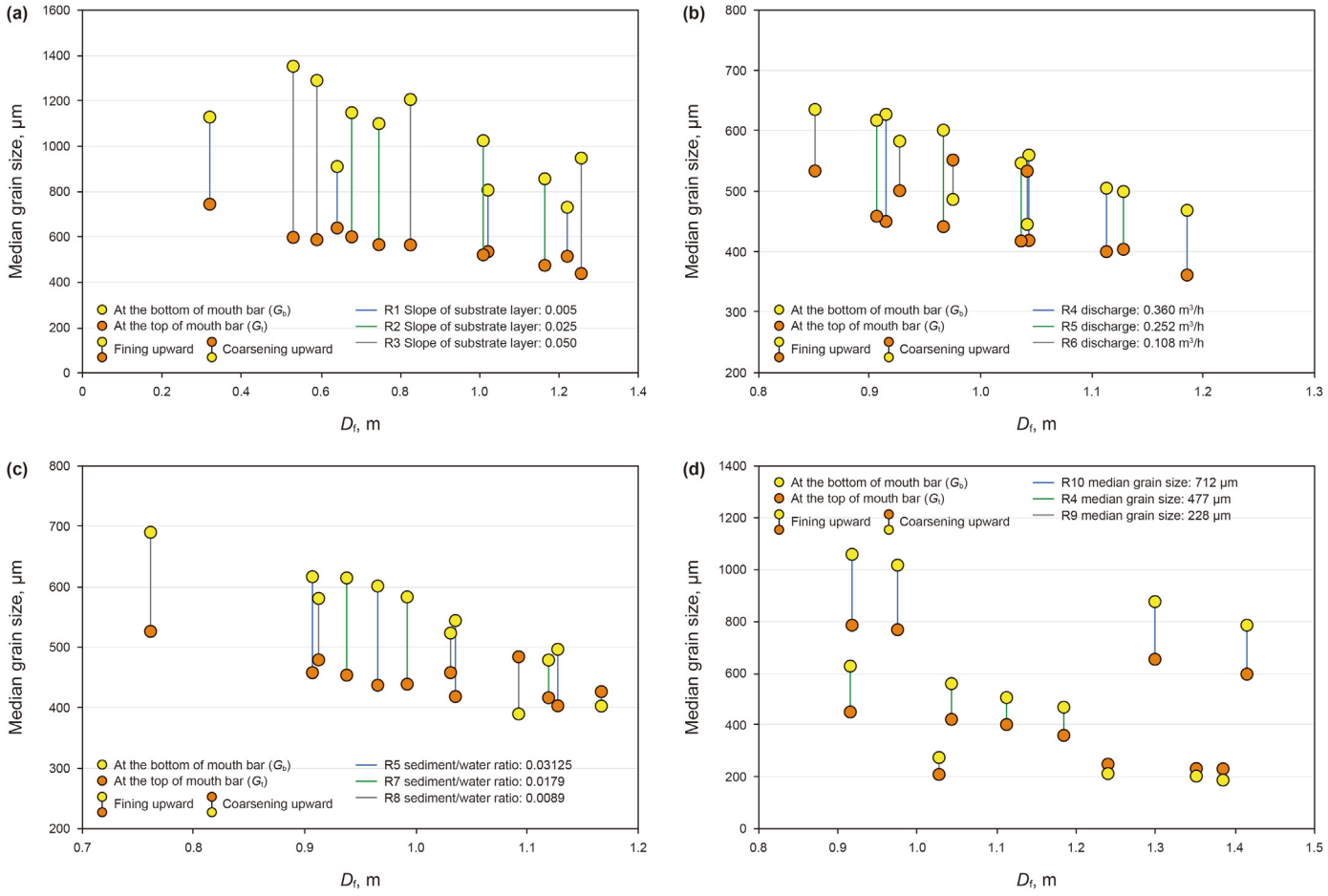

Fig. 6. The grain size distribution along foreset bedding for experiments. As the D_f gradually increases, both median grain size of samples and its range show a decreasing trend within the fining-upward foresets, whereas the range of median grain size increases slightly within the coarsening-upward foresets. The grain size range of mouth bar increases with the increase of slope of substrate layer, discharge, sediment/water ratio and median grain size of sediment supplied.

either fining-upward trend or coarsening-upward trend in fact when the foreset bedding gradients were between 15° and 18° (Fig. 12). Hence, we can conclude that the gradient of the foreset bedding can quantitively describe the vertical grain-size trend of mouth bar. Additionally, early works claimed that the effluent behavior in river-mouth system is associated with the vertical grain-size trend of mouth bar and gradients of foreset bedding (Wright, 1977; Postma, 1990). The friction-dominated effluent diffusion normally caused a gently inclined mouth bar which was less than a few degrees and showed coarsening-upward trend, and the slope of mouth bar may have steepened in the inertia-dominated depositional pattern which is related to the fining-

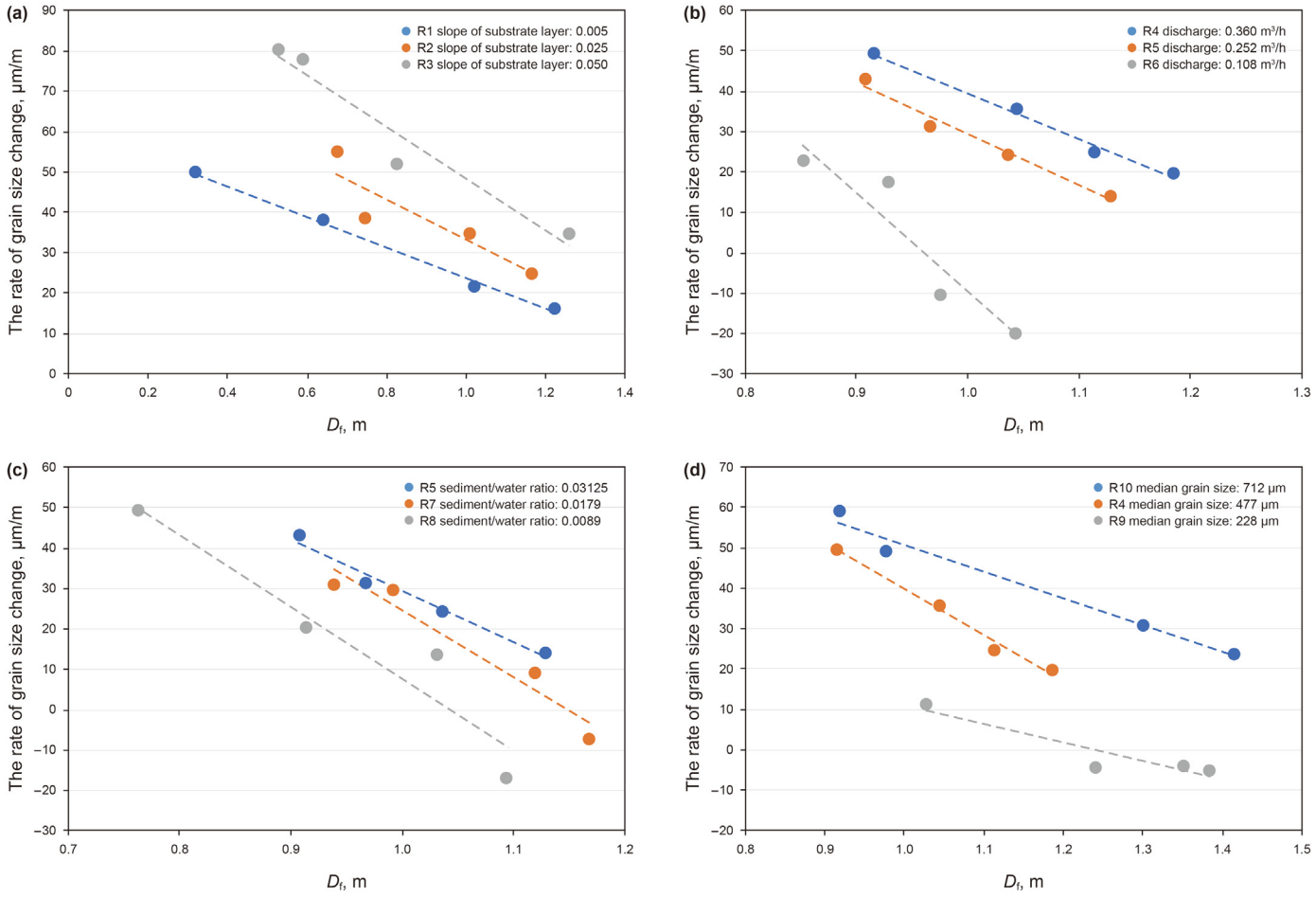

Fig. 7. The rate of grain size change along the foreset bedding for experiments. The rate of grain size change along the foreset bedding shows a decreasing trend as the D_f gradually increases. It also decreases with the decrease of slope of substrate layer, discharge, sediment/water ratio and median grain size of sediment supplied.

upward trend of mouth bar (Fig. 13). It thus can be inferred that steep foreset bedding originated from the strong inertial force, and gentle foreset bedding connected to the strong bed friction.

For homopycnal effluents, the jet structure depends on the ratio of the inertial to viscous forces as indexed by the Reynolds number (*Re*) and the ratio of the inertial forces to gravity as indexed by Froude number (*Fr*) at the river-mouth system (Wright, 1977),

$$Re = v\left(h_0\frac{b_0}{2}\right)^{\frac{1}{2}} / \mu \tag{1}$$

$$Fr = v \Big/ \sqrt{gh_0} \tag{2}$$

where v is the mean outlet velocity, h_0 and b_0 are respectively the depth and width of the channel outlet, and μ is the kinematic viscosity. The inertia-dominated effluent behaved as a fully turbulent jet, while friction-dominated effluent acted as a plane turbulent jet with a pronounced turbulent bed shear. Previous work found that fully turbulent effluent diffusion (inertia-dominated depositional pattern) occurs when *Re* exceeded 2300 or *Fr* exceeded 16.1 (Hayashi et al., 1967). That is, high values of *Re* and *Fr* indicate inertia dominance, but a reduction in the inertia (either *Re* or *Fr*) may cause the friction dominated processes neglecting the influence of buoyant. As shown in Table 4, the values of *Re* greatly exceed 2300 in R1–R5 and R10 experiments, indicating the inertia-dominated effluent at the river-mouth system. The values of *Fr* and *Re* are calculated based on average flow velocity, channel width and depth rather than the instantaneous parameters. Although the values of *Re* are less or close to 2300 in R6–R9 experiments, the effluent behavior is dominated by the bed friction or inertia during mouth bar evolution. Moreover, the value of *Re* was found to decrease with a decrease in the slope of the substrate layer, discharge, sediment/water ratio, and grain size of the sediment supplied, causing a change in effluent behavior from inertia-dominated to friction-dominated at the river-mouth system.

Thus, different slopes of the substrate layer and different feeder systems, such as discharge, sediment/water ratio, and grain size of sediments, controlled the relative strength of inertial force and bed friction. They, in turn, determined the effluent behavior in the river-

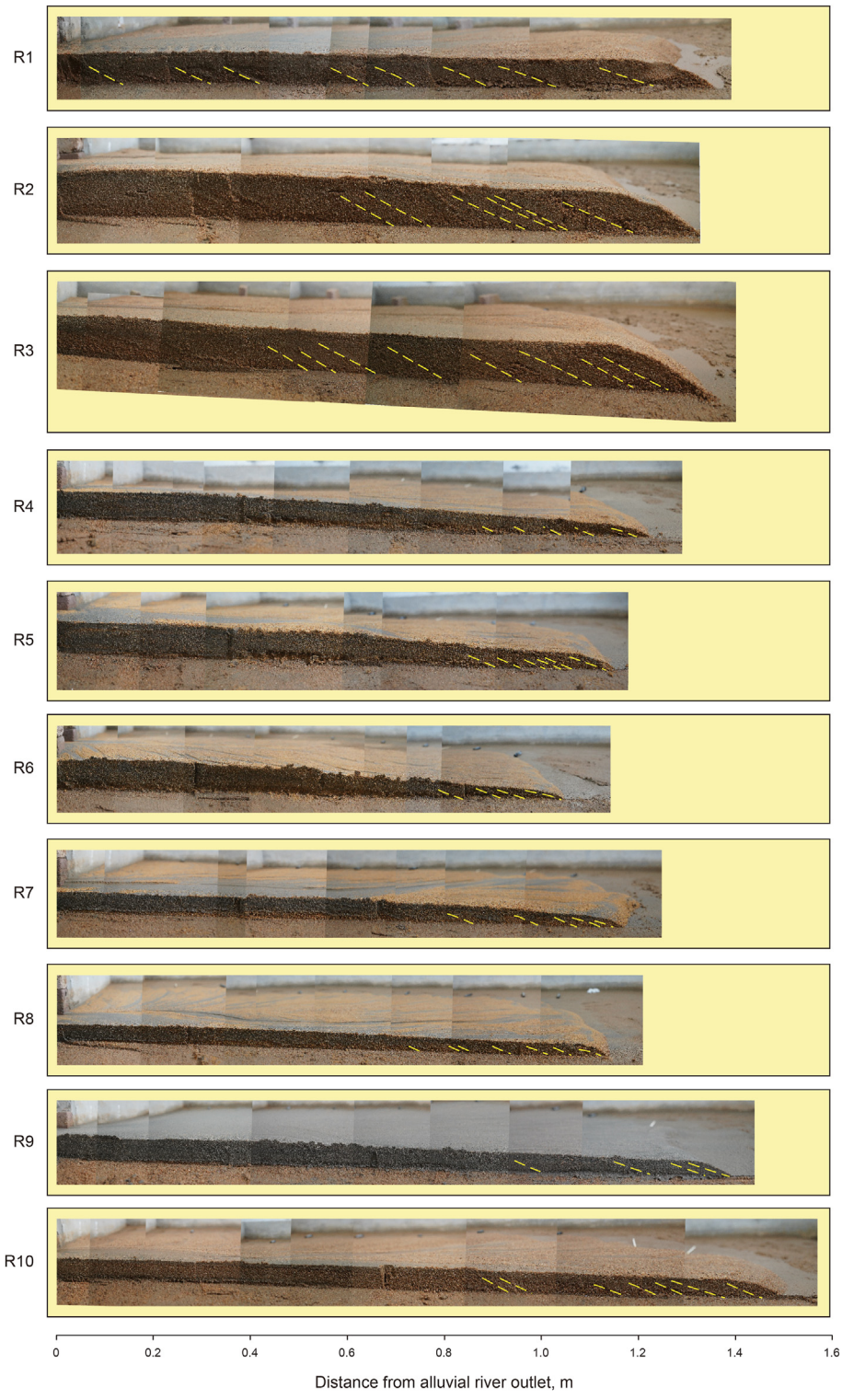

Fig. 8. The fan delta profiles along the centerline for all experimental runs. The yellow lines represent the foreset bedding of mouth bar along the centerline.

mouth system, and further resulted in the vertical grain-size trend of mouth bar and gradients of foreset bedding. This pattern explains the results from Figs. 6 and 10. The fining-upward mouth bar with a steeper gradient of foreset bedding and apparent differences in the range of grain size distribution was deposited in experiments with steeper slope of substrate layer, greater discharge, higher sediment/water ratio and coarser sediment, because effluent was dominated by strong inertia. Decreasing with the inertia and increasing with bed shear stresses, mouth bar in experiment with gentler slope of substrate layer, smaller discharge, lower sediment/water ratio and finer sediment tend to show coarsening-upward trend dominated by the friction-dominated effluent. The gentler

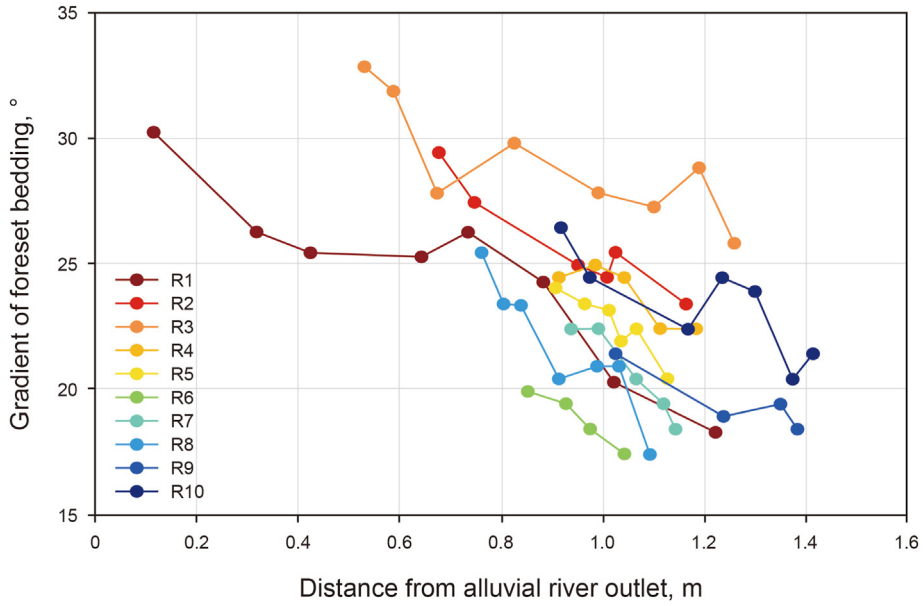

Fig. 9. The relationship between distance from alluvial river outlet and gradient of foreset bedding. The gradients of foreset bedding show a decreasing trend with the evolution of fan delta.

Table 3
Gradients variation of foreset bedding for experiments.

Experiment	Gradient of foreset bedding, °		
	Maximum	Minimum	Average
R1	30.28	18.29	24.56
R2	29.43	23.43	25.84
R3	32.86	25.86	29.04
R4	24.93	22.43	23.73
R5	24.03	20.43	22.56
R6	19.93	17.43	18.81
R7	22.43	18.43	20.63
R8	25.43	17.43	21.7
R9	21.43	18.43	19.56
R10	26.43	21.43	23.36

foreset bedding and greater differences in the range of grain size distribution were both originated from the stronger bed friction.

4.2. Validating the small-scale flume tank models through natural example

There is a growing corpus of detailed outcrop studies of deltas, where there are good delta foreset angles (either explicitly provided, or can be determined from the published data) and grain size data available, with which these results about vertical grain-size trend of mouth bar could be tested. Field observation survey carried by Billi et al. (1991) revealed that coarsening-upward sequences of mouth bar consisted of basal thin beds, dipping basinward by 5°–10° in Pleistocene lacustrine fan delta deposits of the Valdarno Basin, Italy. The mouth bar sandstone units are internally composed of multiple inverse graded bedsets in the Eocene Green River Formation, Uinta Basin, Utah, and the clinoform surfaces of mouth bar have an inclination of 4°–6°, exceptionally up to 14° (Schomacker et al., 2010). The outcrop study of Maestrat Basin in Eastern Spain showed that successions with steeper clinothems displayed fining-upward trend, and the mouth bar accretion surfaces dip up to 24°. Clinothem with low angle show overall coarsening-upward trend (Cole et al., 2021). The subaqueous part of lacustrine fan-deltaic successions is normally graded, with foresets bed inclinations of up to 30° in the Pliocene-Pleistocene Mugello Basin, Central Italy (Benvenuti, 2003). All these previous results confirm that the relationship between vertical grain-size trend of mouth bar and slope of foreset bedding and the cut-off of 15°–18° are applicable for the natural systems. Additionally, they indicated that coarsening-upward clinothems were dominated by cross-bedded sandstone in mouth bar successions. In contrast, the successions, dominated by massive sandstone or massive conglomerate, displayed a fining-upward trend (Cole et al., 2021). The cross-bedded sandstone characterized down-clinothem fining (coarsening-upward trend) is more supportive of waning tractional flow and is indicative of rapid bedload deposition. Sediments are transported by rolling or suspension in traction flow, where high bed shear stresses is dominant, which is in keeping with friction-dominated effluent diffusion. While massive sandstone displaying fining-upward trend likely represent gravity flow, especially turbidity currents. The turbidity currents are considered as fluidal flows in which sediment is supported by fully turbulent flows (Shanmugam, 1996), which is the main jet behavior in inertia-dominated effluent diffusion. Thus, this explained why mouth bars displaying different vertical grain-size trend show different sedimentary structures.

4.3. Further implications for petroleum exploration and development

As mentioned, the high-discharge events, high sediment/water ratio of effluent currents, and coarse-grained flood, the fining-upward mouth bar deposits could be expected given the steep margin of the basin. However, it may be confused with the distributary-channel facies. Hence, caution is needed in the interpretation of ancient fan deltaic rock records. In particular, one needs to (1) identify the depositional setting (such as paleoslope and paleocurrent analysis and grain-size analysis) for inferring the depositional process in the river-mouth system. This lays the foundation for determining whether a fining-upward mouth bar has been developed in the study area or not. One also needs to (2) analyze the plane geometry of sandbodies (lobe or striped shape)

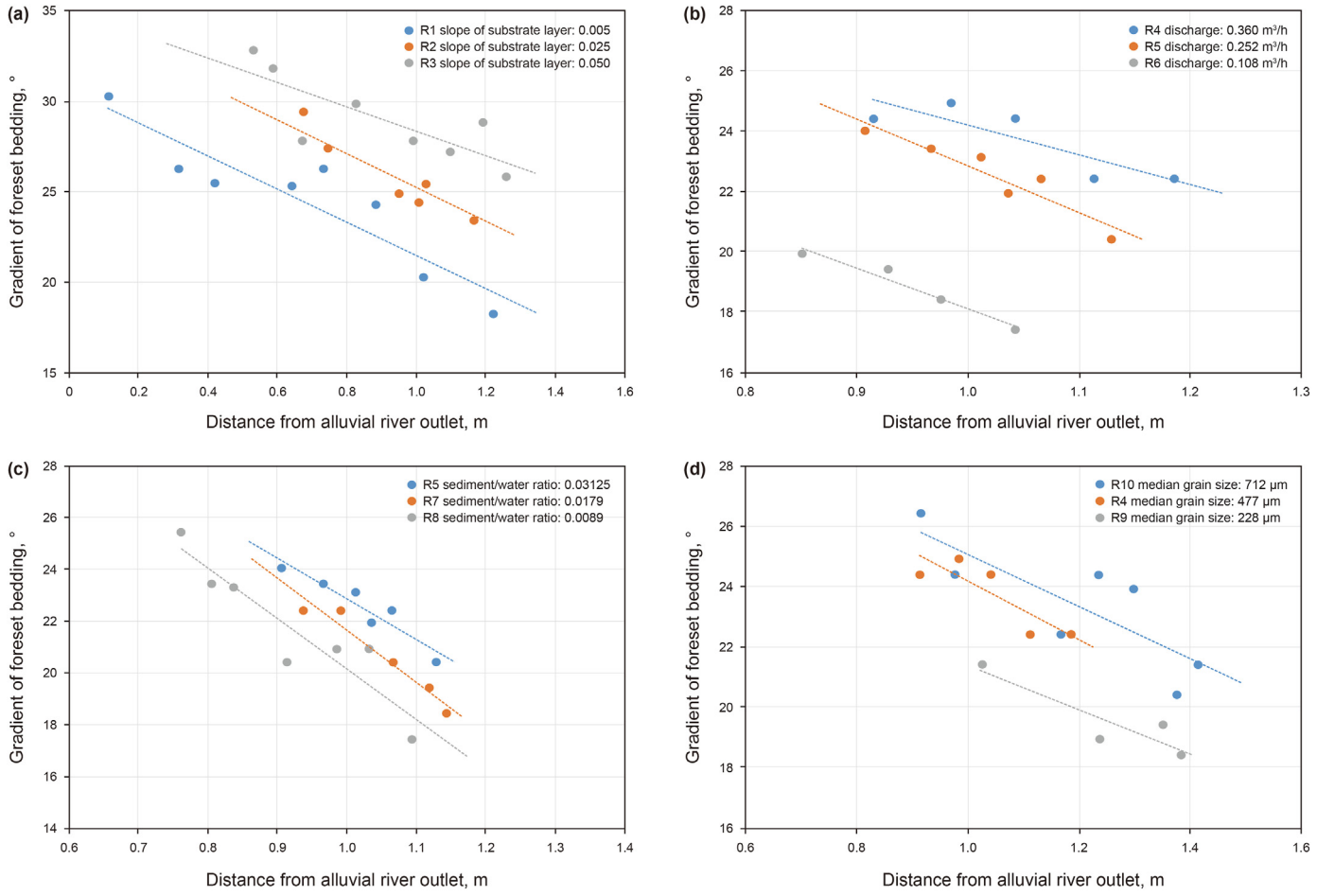

Fig. 10. Gradients variation of foreset bedding for experiments with different tectonic conditions and feeder systems. a: The gradients of foreset bedding increase with increasing slope of substrate layer from 0.005 to 0.050. b: Gradients of foreset bedding decrease with decreasing discharge from 0.360 to 0.108 m^3/h. c: Gradients of foreset bedding decrease with decreasing sediment/water ratio from 0.03125 to 0.0089. d: Gradients of foreset bedding decrease with decreasing median grain size from 712 to 228 μm.

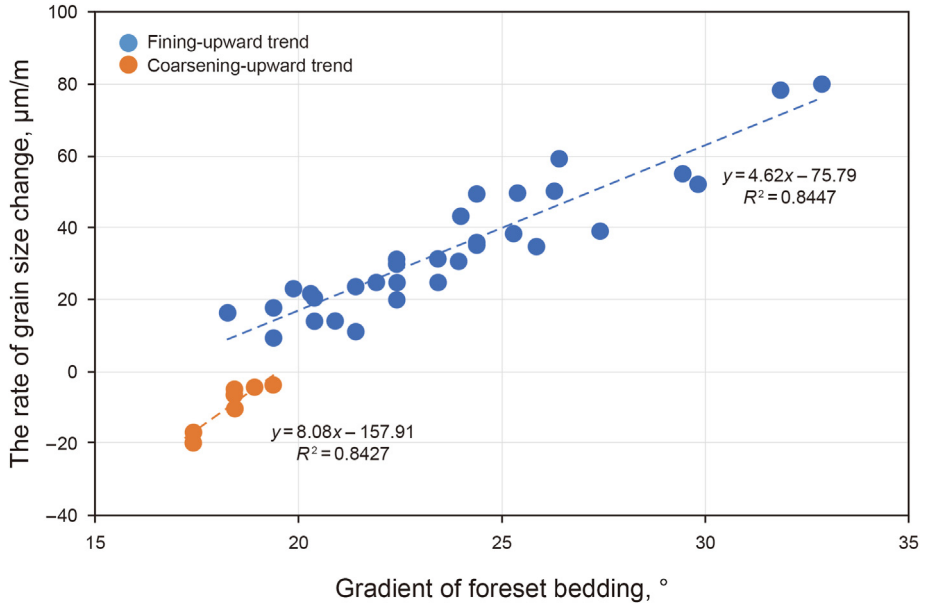

Fig. 11. The positive relationship between gradient of foreset bedding and the rate of grain size change. The foreset bedding gradients are less than 20° within coarsening-upward trend of mouth bar, whereas the gradients are mainly greater than 20° within fining-upward trend of mouth bar.

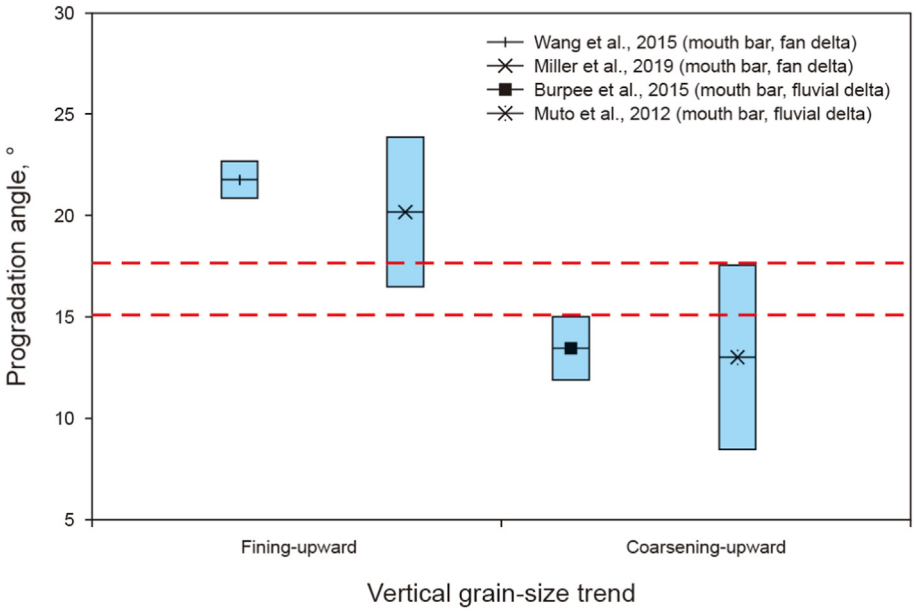

Fig. 12. The relationship between the range of foreset bedding gradient and grading sequence of mouth bar. The blue rectangles represent the range of foreset bedding gradient. Mouth bars with low angle foresets (gentler than 15°) are associated with coarsening-upward profiles, whereas mouth bars with steep foresets (steeper than 18°) are associated with fining-upward successions.

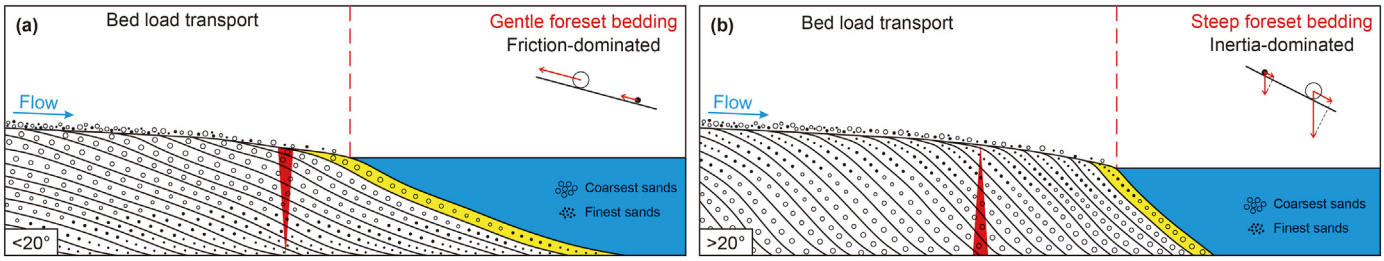

Fig. 13. Friction-dominated and inertia-dominated depositional pattern. The friction-dominated effluent diffusion normally caused a gently inclined mouth bar which was less than a few degrees and showed coarsening-upward trend, and the gradient of mouth bar may steepen in inertia-dominated depositional pattern which is related to the fining-upward trend of mouth bar.

Table 4
The value of *Fr* and *Re* of feeder system.

Experiment	Flow velocity of feeder system, $m \cdot s^{-1}$	*Fr*	*Re*
R1	0.1	0.224	4000
R2	0.1	0.224	4000
R3	0.1	0.224	4000
R4	0.1	0.224	3076
R5	0.07	0.157	2154
R6	0.03	0.067	924
R7	0.09	0.20	2770
R8	0.12	0.26	3692
R9	0.1	0.224	2222
R10	0.1	0.224	4000

combined with abundant data to distinguish the fining-upward mouth bar from distributary channels.

5. Conclusions

This study conducted flume experiments to elucidate the mechanism and controlling factors of the vertical grain-size trend of a mouth bar of a fan delta.

First, we found that the mouth bars of fan delta mostly show the fining-upward trend in experiments, whereas only a few columns in R6–R9 show the coarsening-upward trend. As the D_f gradually increases, both median grain size and the range of it show a decreasing trend within the fining-upward foresets, whereas the range of median grain size slightly increases within the coarsening-upward foresets. Moreover, the grain-size range of mouth bar increases with the increase of slope of substrate layer, discharge, sediment/water ratio and median grain size of sediment supplied.

Second, we identified that the different slopes of the substrate layer and different feeder systems controlled the relative strength of inertial force and bed friction. In turn, they determined the effluent behavior in the river-mouth system, and consequently yielded the different vertical grain-size trend of mouth bar and slopes of foreset bedding. The fining-upward mouth bar with steeper gradient of foreset bedding and apparent differences in the range of grain size distribution deposited in experiments with steeper slope of substrate layer, greater discharge, higher sediment/water ratio and coarser sediment, because effluent was dominated by strong inertia. Decreasing with the inertia and increasing with bed shear stresses, mouth bar in experiment with gentler slope of substrate layer, smaller discharge, lower sediment/water ratio and finer sediment tend to show coarsening-upward trend dominated by the friction-dominated effluent. The gentler foreset bedding and

greater differences in the range of grain size distribution were shown to be originated from the stronger bed friction.

Third, we validated the interpretations from small-scale flume tank models by using natural examples. The relationship between vertical grain-size trend of mouth bar and slope of foreset bedding and the cut-off of 15°–18° are applicable in natural systems. Overall, we outlined two steps for effective interpretation of ancient fan deltaic rock records, where fining-upward mouth bar deposits may be misinterpreted with distributary-channel facies. These two steps include the identification of the depositional setting, while inferring the depositional processes in the river-mouth system, and the analysis of the plane geometry of sandbodies.

Acknowledgment

This project was supported by the National Natural Science Foundation of China (No. 41772101).

References

Ambrosetti, E., Martini, I., Sandrelli, F., 2017. Shoal-water deltas in high-accommodation settings: insights from the lacustrine Valimi formation (Gulf of Corinth, Greece). Sedimentology 64 (2), 425–452. https://doi.org/10.1111/sed.12309.

Arndorfer, D., 1973. Discharge patterns in two crevasses of the Mississippi River Delta. Mar. Geol. 15, 269–287. https://doi.org/10.1016/0025-3227(73)90074-1.

Benvenuti, M., 2003. Facies analysis and tectonic significance of lacustrine fan-deltaic successions in the Pliocene–Pleistocene Mugello Basin, Central Italy. Sediment. Geol. 197–234. https://doi.org/10.1016/S0037-0738(02)00234-8, 2003.

Bhattacharya, J.P., Willis, B.J., 2001. Lowstand deltas in the frontier formation, powder river basin, Wyoming: implications for sequence stratigraphic models. AAPG (Am. Assoc. Pet. Geol.) Bull. 85 (2), 261–294. https://doi.org/10.1306/8626C7B7-173B-11D7-8645000102C1865D.

Billi, P., Magi, M., Sagri, M., 1991. Pleistocene lacustrine fan delta deposits of the Valdarno Basin, Italy. J. Sediment. Petrol. 61, 280–290. https://doi.org/10.1306/D42676EF-2B26-11D7-8648000102C1865D.

Bressan, G.S., Kietzmann, D.A., Palma, R.M., 2013. Facies analysis of a Toarcian–Bajocian shallow marine/coastal succession (Bardas Blancas formation) in northern Neuquén basin, Mendoza province, Argentina. J. S. Am. Earth Sci. 43, 112–126. https://doi.org/10.1016/j.jsames.2013.01.007.

Burpee, A.P., Slingerland, R.L., Edmonds, D.A., et al., 2015. Grain-size controls on the morphology and internal geometry of river-dominated deltas. J. Sediment. Res. 85, 699–714. https://doi.org/10.2110/jsr.2015.39.

Caldwell, R.L., Edmonds, D.A., 2014. The effects of sediment properties on deltaic processes and morphologies: a numerical modeling study. J. Geophys. Res.: Earth Surf. 118, 961–982. https://doi.org/10.1002/2013JF002965.

Carvalho, A.H., Vesely, F.F., 2017. Facies relationships recorded in a Late Paleozoic fluvio-deltaic system (Paraná Basin, Brazil): insights into the timing and triggers of subaqueous sediment gravity flows. Sediment. Geol. 352, 45–62. https://doi.org/10.1016/j.sedgeo.2016.12.004.

Cole, G., Jerrett, R., Watkinson, M.P., 2021. A stratigraphy example of the architecture and evolution of shallow water mouth bars. Sedimentology 68, 1227–1254. https://doi.org/10.1111/sed.12825.

Coleman, J.M., Gagliano, S.M., Webb, J.E., 1964. Minor sedimentary structures in a prograding distributary. Mar. Geol. 1, 240–258. https://doi.org/10.1016/0025-3227(64)90062-3.

Edmonds, D.A., Slingerland, R.L., 2007. Mechanics of river mouth bar formation: implications for the morphodynamics of delta distributary networks. J. Geophys. Res. 112, F02034. https://doi.org/10.1029/2006JF000574.

Edmonds, D.A., Slingerland, R.L., 2010. Significant effect of sediment cohesion on delta morphology. Nat. Geosci. 3, 105–109. https://doi.org/10.1038/NGEO730.

Fabbricatore, D., Robustelli, G., Muto, F., 2014. Facies analysis and depositional architecture of shelf-type deltas in the Crati Basin (Calabrian arc, south Italy). Ital. J. Geosci. 133 (1), 131–148. https://doi.org/10.3301/IJG.2013.19.

Fagherazzi, S., Edmonds, D.A., Nardin, W., et al., 2015. Dynamics of river mouth deposits. Rev. Geophys. 53 (3), 642–672. https://doi.org/10.1002/2014RG000451.

Fielding, C., Trueman, J., Alexander, J., 2005. Sharp-based, flood-dominated mouth bar sands from the Burdekin River Delta of Northeastern Australia: extending the spectrum of mouth-bar facies, geometry, and stacking patterns. J. Sediment. Res. 75, 55–66. https://doi.org/10.2110/jsr.2005.006.

García-García, F., Fernández, J., Viseras, U., et al., 2006. Architecture and sedimentary facies evolution in a delta stack controlled by fault growth (Betic Cordillera, southern Spain, late Tortonian). Sediment. Geol. 185, 79–92. https://doi.org/10.1016/j.sedgeo.2005.10.010.

Hayashi, J., Shuto, N., Kawakami, K., 1967. Basic study on the diffusion of warm water jets discharged from power plants into bays. Coast. Eng. Jpn. 10 (1), 129–142. https://doi.org/10.1080/05785634.1967.11924061.

Hoyal, D.C.J.D., Sheets, B.A., 2009. Morphodynamic evolution of experimental cohesive deltas. J. Geophys. Res. 114, F02009. https://doi.org/10.1029/2007JF000882.

Ilgar, A., Nemec, W., 2005. Early Miocene lacustrine deposits and sequence stratigraphy of the Ermenek Basin, central Taurides, Turkey. Sediment. Geol. 173, 233–275. https://doi.org/10.1016/j.sedgeo.2003.07.007.

Jia, H.B., Ji, H.C., Wang, L.S., et al., 2018. Controls of a Triassic fan-delta system, Junggar basin, NW China. Geol. J. 53, 3093–3109. https://doi.org/10.1002/gj.3147.

Lai, J., Wang, G.W., Fan, Z.Y., et al., 2017. Sedimentary characterization of a braided delta using well logs: the upper Triassic Xujiahe formation in Central Sichuan basin, China. J. Petrol. Sci. Eng. 154, 172–193. https://doi.org/10.1016/j.petrol.2017.04.028.

Leila, M., Moscariello, A., 2019. Seismic stratigraphy and sedimentary facies analysis of the pre- and syn- Messinain salinity crisis sequences, onshore Nile Delta, Egypt: implications for reservoir quality prediction. Mar. Petrol. Geol. 101, 303–321. https://doi.org/10.1016/j.marpetgeo.2018.12.003.

Miller, K.L., Kim, W., McElory, B., 2019. Laboratory investigation on effects of flood intermittency on fan delta dynamics. J. Geophys. Res.: Earth Surf. 124, 383–399. https://doi.org/10.1029/2017JF004576.

Muto, T., Yamagishi, C., Sekiguchi, T., et al., 2012. The hydraulic autogenesis of distinct cyclicity in delta foreset bedding: flume experiments. J. Sediment. Res. 82, 545–558. https://doi.org/10.2110/jsr.2012.49.

Mutti, E., Tinterri, R., Di Biase, D., et al., 2000. Delta front associations of ancient flood-dominated fluvio-deltaic systems. Rev. Soc. Geol. Espana 13, 165–190.

Nian, T., Jiang, Z.X., Wang, G.W., et al., 2018. Characterization of braided river-delta facies in the Tarim Basin Lower Cretaceous: application of borehole image logs with comparative outcrops and cores. Mar. Petrol. Geol. 97, 1–23. https://doi.org/10.1016/j.marpetgeo.2018.06.024.

Paola, C., Twilley, R.R., Edmonds, D.A., et al., 2011. Natural processes in delta restoration: application to the Mississippi Delta. Ann. Rev. Mar. Sci 3, 37–91. https://doi.org/10.1146/annurev-marine-120709-142856.

Postma, G., 1990. An analysis of the variation in delta architecture. Terra Rev. 2, 124–130. https://doi.org/10.1111/j.1365-3121.1990.tb00052.x.

Rasmussen, H., 2000. Nearshore and alluvial facies in the Sant Llorenc del Munt depositional system: recognition and development. Sediment. Geol. 138, 71–98. https://doi.org/10.1016/S0037-0738(00)00144-5.

Rohais, S., Eschard, R., Guillocheau, F., 2008. Depositional model and stratigraphic architecture of rift climax Gilbert-type fan deltas (Gulf of Corinth, Greece). Sediment. Geol. 210, 132–145. https://doi.org/10.1016/j.sedgeo.2008.08.001.

Schomacker, E.R., Kjemperud, A.V., Nystuen, J.P., et al., 2010. Recognition and significance of sharp-based mouth-bar deposits in the Eocene Green River formation, Uinta Basin, Utah. Sedimentology 57, 1069–1087. https://doi.org/10.1111/j.1365-3091.2009.01136.x.

Schuurman, F., Marra, W.A., Kleinhans, M.G., 2013. Physics-based modeling of large braided sand-bed rivers: bar pattern formation, dynamics, and sensitivity. J. Geophys. Res.: Earth Surf. 118, 2509–2527. https://doi.org/10.1002/2013JF002896.

Shanmugam, G., 1996. High-density turbidity currents: are they sandy debris flows? J. Sediment. Res. 66 (1), 2–10. https://doi.org/10.1306/D426828E-2B26-11D7-8648000102C1865D.

Shultz, A.W., 1984. Subaerial debris-flow deposition in the upper paleozoic cutler formation, western Colorado. J. Sediment. Res. 54 (3), 759–772. https://doi.org/10.1306/212F84EF-2B24-11D7-8648000102C1865D.

Tye, R.S., Coleman, J.M., 1989. Depositional processes and stratigraphy of fluvially dominated lacustrine deltas: Mississippi Delta Plain. J. Sediment. Geol. 59 (6), 973–996. https://doi.org/10.1306/212F90CA-2B24-11D7-8648000102C1865D.

Van Dijk, M., Postma, G., Kleinhans, M.G., 2009. Autocyclic behaviour of fan deltas: an analogue experimental study. Sedimentology 56, 1569–1589. https://doi.org/10.1111/j.1365-3091.2008.01047.x.

Van Heerden, I.L., Roberts, H.H., 1988. Facies development of Atchafalaya Delta, Louisiana: a modern bayhead delta. Bulletin 72, 439–453. https://doi.org/10.1306/703C8EB1-1707-11D7-8645000102C1865D.

Wang, J.H., Jiang, Z.X., Zhang, Y.F., et al., 2015. Flume tank study of surface morphology and stratigraphy of a fan delta. Terra. Nova 27, 42–53. https://doi.org/10.1111/ter.12131.

Weckwerth, P., 2018. Fluvial responses to the Weichselian ice sheet advances and retreats: implications for understanding river paleohydrology and pattern changes in Central Poland. Int. J. Earth Sci. 107, 1407–1429. https://doi.org/10.1007/s00531-017-1545-y.

Wright, L.D., 1977. Sediment transport and deposition at river mouths: a synthesis. Geol. Soc. Am. Bull. 88, 857–868. https://doi.org/10.1130/0016-7606(1977)88<857:STADAR>2.0.CO;2.

Wright, L.D., Coleman, J.M., 1974. Mississippi River mouth processes: effluent dynamics and morphologic development. J. Geol. 82, 751–778. https://doi.org/10.1086/628028.

Wu, W., Li, Q., Pei, J.X., et al., 2020. Seismic sedimentology, facies analyses, and high-quality reservoir predictions in fan deltas: a case study of the Triassic Baikouquan Formation on the western slope of the Mahu Sag in China's Junggar Basin. Mar. Petrol. Geol. 120, 104546. https://doi.org/10.1016/j.marpetgeo.2020.104546.

Xu, C.M., Gehenn, J.M., Zhao, D.H., et al., 2015. The fluvial and lacustrine sedimentary systems and stratigraphic correlation in the Upper Triassic Xujiahe

Formation in Sichuan Basin, China. AAPG (Am. Assoc. Pet. Geol.) Bull. 99 (11), 2023–2041. https://doi.org/10.1306/07061514236.
Zavala, C., Pan, S.X., 2018. Hyperpycnal flows and hyperpycnites: origin and distinctive characteristics. Lithologic Reservoirs 30 (1), 1–18. https://doi.org/10.3969/j.issn.1673-8926.2018.01.001 (in Chinese).
Zhang, K., Wu, S.H., Feng, W.J., et al., 2020. Bar dynamics in a sandy braided river: insights from sediment numerical simulations. Sediment. Geol. 396, 105557. https://doi.org/10.1016/j.sedgeo.2019.105557.
Zhang, K., Wu, S.H., Feng, W.J., et al., 2021. Experimental study of fan delta evolution: autogenic cycles of fully confined channelized flow and small secondary channelized flows. Sediment. Geol. 426, 106024. https://doi.org/10.1016/j.sedgeo.2021.106024.
Zhang, X.F., Wang, S.Q., Wu, X., et al., 2016. The development of a laterally confined laboratory fan delta under sediment supply reduction. Geomorphology 257, 120–133. https://doi.org/10.1016/j.geomorph.2015.12.027.